A STOCHASTIC MODEL OF REGIONAL CEREBRAL CIRCULATION

B. Hoop, Jr., R. G. Ojemann, and G. L. Brownell

Massachusetts General Hospital, Boston, Massachusetts

Characteristics of regional cerebral circulation in man are often studied with radionuclide-labeled tracers using extracranial detection techniques. Most investigations have used diffusible compounds since measurements made with nondiffusible substances, i.e., substances which do not diffuse through the vascular walls, have yielded indices of circulation times rather than values of regional blood flow (*1,2* and references therein).

Clinical measurements of regional cerebral circulation in man have been made by extracranial monitoring of the passage of a nondiffusible radionuclide-labeled tracer through six regions of a cerebral hemisphere following intracarotid bolus injection. Details of the clinical method and measurements are discussed in the foregoing report (*3*). The data obtained in normal subjects are compared with a stochastic model of regional cerebral circulation based upon the assumption of a random walk of tracer through regions of the cerebral vascular bed.

Within the limits of applicability of the model, the analysis provides normal values of regional cerebral blood flow (rCBF) per monitored vascular volume and regional cerebral vascular volume (rCBV), as well as normal values of rCBF per volume of tissue monitored.

METHOD

Regional impulse response function*. Figure 1A shows a schematic representation of a single detection field of view defining approximately 70–100 cm^3 of tissue in a cerebral hemisphere (*3*). The mathematical function which characterizes the motion of tracer exclusively within a monitored region is often called the impulse response function or the frequency function of transit times, $h(\tau)$ (*5*). Several investigators (*5–8*) have restated the fundamental relationship that the product of the mean transit time [centroid or first moment of $h(\tau)$ about the time ($\tau = 0$)† of impulse injection into the region] and the tracer flow rate F through the region is equal to the volume V. It has often been emphasized (*9*) that V is the volume throughout which the tracer is distributed. In the case of a nondiffusible tracer which is distributed only within the vascular compartment, this volume V is equal to the volume of the vascular bed traversed by the tracer.

Zierler (*9*) has pointed out that the method of external monitoring of tracer activity in V does not directly provide a measurement of the impulse response function for V.

An elementary stochastic model of nondiffusible tracer flow through a regional volume V of a vascular bed is based on a one-dimensional random walk process in which the tracer is assumed to be carried by the tracee with an average linear velocity of flow u through a uniform vascular labyrinth of mean path length b and is simultaneously dispersed along this path length by stochastic or random collisions with the labyrinth (*10,11*). The dispersion of tracer throughout the labyrinth volume is described by a diffusion coefficient D.

Diffusion is to be understood here as the dispersion of tracer within the vascular bed by the vascular labyrinth and is not to be confused with the concept of "nondiffusible" tracer.

If it is further assumed that there is continuity of tracer flow at all points in the labyrinth and that

* Unless otherwise defined, nomenclature used throughout the text is that suggested by a Task Group on Tracer Kinetics in a report requested by the International Commission on Radiation Units and Measurements (*4*).

Received May 7, 1970; revision accepted Feb. 1, 1971.

For reprints contact: Bernard Hoop, Physics Research Laboratory, Massachusetts General Hospital, Boston, Mass. 02114.

† The notation τ is used in this section to designate time measured from the time of injection ($\tau = 0$) *directly* into the regional volume to distinguish from the notation t used in the following sections to designate time measured from intracarotid injection ($t = 0$).

tracer does not return to the labyrinth after once crossing the outflow surface, it can be shown that the current of tracer particles crossing the outflow surface at $x = b$, following an impulse input of a unit amount of tracer across the inflow surface at $x = 0$, $\tau = 0$, is given by (*10,11*),

$$h(\tau) = \left(\frac{b/u}{\kappa^2\pi\tau^3}\right)^{1/2} \exp\left[\frac{b/u}{\kappa^2\tau}\left(1 - \frac{u}{b}\tau\right)^2\right]. \quad (1)$$

This expression is characterized by two parameters: b/u and κ^2. It may be readily verified that the area under $h(\tau)$ is unity and that the mean transit time is simply b/u, the reciprocal of which may be interpreted within the context of the present model as rCBF per monitored vascular volume, as discussed above (*5*).

The quantity κ^2 is related to the diffusion coefficient D by the expression $\kappa^2 = 4D/ub$ (*10*). Using the general definition of the diffusion coefficient from elementary theory of transport phenomena (*12*) and assuming that the mean path length b is equal to the total vascular path traversed by all of the tracer divided by the number of paths into which the tracer has been separated, the quantity $4/3\kappa^2$ can be shown to be equal to the regional vascular volume in the volume of tissue monitored.

Let V_T and V be, respectively, the volume of tissue monitored and the volume of distribution (assumed to be the vascular volume) of tracer within V_T.

If the vascular labyrinth in the monitored volume is represented by a density of small vessel and capillary bifurcations (N bifurcations/V_T) which scatter or disperse the tracer, and if σ is the mean small vessel and capillary cross-sectional area, the mean free path λ, of tracer through the labyrinth (from bifurcation to bifurcation) is given by (*12*) $\lambda = V_T/N\sigma$.

If the mean path length b of tracer through the entire monitored volume V_T is taken to be the total vascular path p traversed by all of the tracer passing through V_T divided by the number N of paths in V_T into which the tracer has been separated ($b = p/N$), then, making use of the expression for the diffusion coefficient (*12*) $D = \lambda u/3$, we may write the total vascular volume V per monitored tissue volume V_T as $V/V_T = p\sigma/V_T = bN\sigma/V_T = b/\lambda = ub/3D = 4/3\kappa^2$. Assuming a distribution of velocities, u alters the factor 4/3. In the present analysis, such a refinement is not warrantable.

The product of u/b and $4/3\kappa^2$ is therefore rCBF in the volume of tissue monitored.

Analysis. Following an intracarotid bolus injection of a nondiffusible tracer at a time $t = 0$, the input of tracer into a monitored cerebral region cannot, in general, be assumed to be an impulse. The regional input of tracer can be characterized by an input function g(t) which describes the motion of tracer in parts of the circulatory bed it traverses before its entrance into the regional volume as well as dispersion of the tracer due to a rapid injection of finite duration (see Fig. 1A). The area under g(t) is equal to the total amount of tracer entering the volume. The current of tracer particles crossing the outflow surface of the monitored regional volume as a function of time is therefore given by the convolution $g(t)*h(t)$ of the input function g(t) with

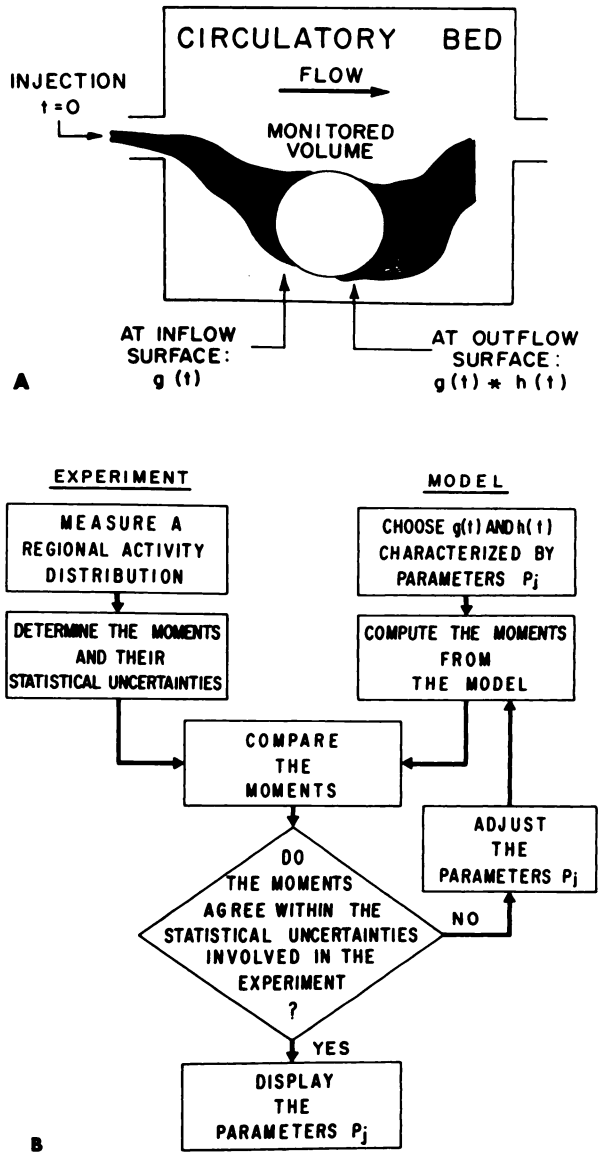

FIG. 1. A is schematic representation of passage of tracer bolus through circulatory bed following injection at time $t = 0$. Current of tracer particles (shaded area) crossing inflow and outflow surfaces of regional monitored volume at time t is g(t) and $g(t)*h(t)$, respectively, where * denotes convolution (9,13). B is general flow diagram of method of analysis of measured regional activity distribution in terms of model expressed by functions g(t) and h(t). Parameters P_j of functions g(t) and h(t) are defined in text.

the impulse response function h(t), where * denotes convolution (*13*).

The total amount of tracer q(t) at time t in the monitored volume is therefore given by (*9*),

$$q(t) = \int_0^t [g(s) - g(s)*h(s)]ds. \qquad (2)$$

If the assumption is made that the observed activity at time t is related to the amount of tracer q(t) in the monitored volume by a constant detection efficiency factor, we can define the normalized moments of q(t), equally valid for the observed activity distribution, which are independent of detection efficiency. The nth order moment μ_n about the intracarotid injection time t = 0 of q(t), normalized to unit area under q(t), is formally expressed as

$$\mu_n = \frac{\int_0^\infty t^n q(t)dt}{\int_0^\infty q(t)dt} \qquad (3)$$

in which the upper limit of integration need only extend to the time when the activity returns to a small, flat background (*3*).

Since q(t) goes to zero more rapidly than $t^{-(n+1)}$ as t increases indefinitely, by extension of the arguments used by Meier and Zierler (*5*), one may substitute Eq. 2 into Eq. 3 and integrate by parts to obtain an expression for the normalized nth order moment μ_n of q(t) in terms of the moments of g(t) and h(t); i.e.,

$$\mu_n = \frac{1}{n+1} \sum_{i=1}^{n+1} \frac{(n+1)!}{i!(n+1-i)!} \frac{\eta_i}{\eta_1} \frac{\zeta_{(n+1-i)}}{\zeta_0} \qquad (4)$$

in which ζ_n and η_n are the nth order moments about the intracarotid injection time t = 0 of g(t) and h(t), respectively. The zero order moment or area under g(t) is designated by ζ_0. Hence the normalized moments of g(t) appear explicitly in Eq. 4, which indicates that the expressions Eq. 3 and Eq. 4 are independent of the amount of tracer entering the monitored volume.

It is by means of the expressions Eq. 3 and Eq. 4 that the experimental data are compared with the model represented by the functions g(t) and h(t).

This comparison is accomplished as outlined in the flow diagram shown in Fig. 1B. In the clinical investigation (*3*), a measurement of a regional activity distribution is obtained. Moments of each of the measured activity distributions are computed

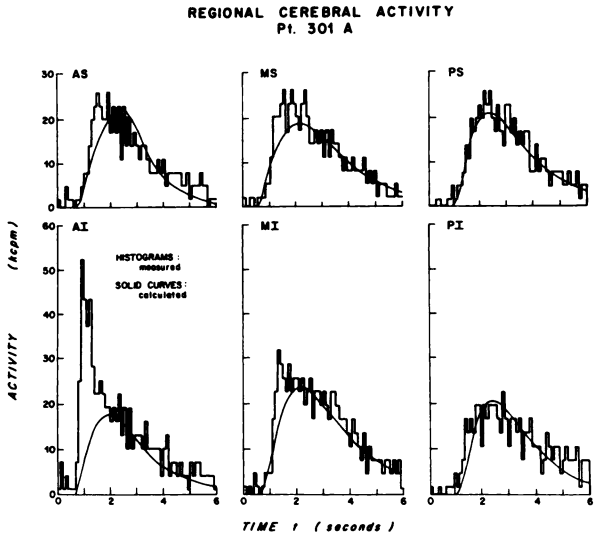

FIG. 2. Activity distributions measured in three superior (S) and inferior (I) regions [anterior (A), middle (M), and posterior (P)] of left cerebral hemisphere of 55-year-old male patient with normal angiogram following rapid intracarotid bolus injection at time t = 0 of 1-ml bolus of 500 μCi of ^{99m}Tc-sodium pertechnetate. Activity in kcpm as counts accumulated in 0.1-sec intervals is plotted as histograms vs. time in seconds after correction for flat background. Shown for comparison are solid curves calculated as explained in text.

from Eq. 3 and compared by an iterative least-squares method with moments calculated from Eq. 4 using the moments of the assumed functional forms for h(t) and g(t). The impulse response function h(t) of the monitored region is represented by Eq. 1. The same functional form is used to represent the input function g(t). The parameters characterizing h(t) and g(t) are varied systematically until an overall squared error of fit E^2 is minimized. Similar methods are often used, for example, in the analysis of nuclear scattering data (*14*).

In the iterative least-squares procedure, E^2 is treated as a function of the parameters $(P_1, \ldots, P_M)$ of g(t) and h(t), in which M is the total number of parameters contained in the functional forms of g(t) and h(t). From an initially chosen set of parameters, an initial value of E^2 is computed. Each parameter P_j is changed by an amount proportional to the gradient of E^2 with respect to P_j, and E^2 is recomputed. The procedure is reiterated until E^2 is minimized.

The success of the iterative least-squares method depends upon the initial choice of parameters and upon the statistical quality of the experimental data, as well as upon the applicability of the model. As described in a preliminary report (*15*), the four parameters (M = 4) used in the present analysis are the quantities b/u and κ [= $(4D/ub)^{1/2}$] of the functions g(t) and h(t) represented by the functional form given in Eq. 1. Initial values of these

parameters were chosen from values lying in the range of $0.5 < \kappa < 2.0$ and $0.5 \text{ sec} < b/u < 3.5$ sec. Initial values of the parameters lying within these ranges yielded values of the first five order moments $\mu_1, \ldots . \mu_5$ (Eq. 4) which were of the order of magnitude of experimentally determined moments (Eq. 3). Several initially chosen sets of parameters used in the iterative least-squares analysis of a given activity distribution yielded satisfactory values of the final overall squared error of fit E^2 and final values of a given parameter generally lying within ±10% of each other. In the analysis of a single regional activity distribution obtained in the present clinical experiment (*3*) using a single initially chosen set of parameters, it is estimated that b/u and κ are determined with uncertainties of approximately ±4% and ±9%, respectively.

The data recording and processing system used in the present analysis has been described elsewhere (*3,16,17*). The practicability of the analytical method is illustrated in Fig. 2. Activity distributions measured in six regions of the left cerebral hemisphere of a 55-year-old patient with a normal angiogram are shown by the histogram plots in Fig. 2. Activity as counts accumulated in 0.1-sec intervals is plotted against time following intracarotid bolus injection. The plotted activity distributions have been corrected for an average flat background determined from regional activity measured between 15 and 20 sec after injection. Also shown in Fig. 2 are regional tracer distributions q(t) calculated from Eq. 2. In the calculation of the distributions q(t), values of the parameters b/u and κ of the functions g(t) and h(t) were used, which resulted in a best comparison of the measured moments (Eq. 3) with moments of q(t) calculated from Eq. 4. Each of the calculated distributions shown in Fig. 2 have been normalized to the respective measured activity distributions between 2.5 and 5 sec. Values of the calculated moments, resulting in the most favorable comparison with the measured moments, were within the statistical uncertainties in the measured moments in all regions except the anterior inferior (AI) region. The prominent peak in the measured AI activity distribution is due to the passage of the injected bolus through the carotid siphon and intracranial portion of the internal carotid artery within the AI region. The measured AI activity distributions could not be satisfactorily represented by the model chosen in the present analysis. Similar contributions to the activity distributions in other regions (e.g., AS, MI, and MS) are also evident. Since these contributions are not adequately described by the present model, the calculated distributions represent only that portion of the regional cerebral circulation which best satisfies the criteria of the random walk model.

RESULTS

Table 1 summarizes the results obtained from measurements made in 17 normal subjects of mean age 43 years and range 20–63 years. The mean values and standard deviations of rCBF per monitored vascular volume, rCBV per monitored tissue volume, and rCBF per monitored tissue volume in six cerebral regions are given. The mean and standard deviation for all six regions is also given. For comparison with the present work, ranges of values of rCBF per 100 gm tissue (*18,19* and references therein) and of cerebral capillary volume (vol % or $cm^3/100\ cm^3$ tissue) (*20,21*) are given in the last column of Table 1. A range of values for rCBF per vascular volume in 100 cm^3 of tissue, calculated from the above two quantities, is also given (a tissue density of 1 gm/cm^3 is assumed).

Figure 3 shows the behavior of mean rCBF and rCBV as a function of age in the 17 subjects. An

TABLE 1. MEAN VALUES AND STANDARD DEVIATIONS OF rCBF AND rCBV IN 17 NORMAL HUMAN STUDIES

	Cerebral regions*							
	AI	MI	PI	AS	MS	PS	Mean of six regions	Other work
Mean rCBF/vascular volume (ml/min/ml)	29.7 ±2.2	29.3 ±2.4	30.0 ±2.7	29.7 ±1.9	27.8 ±1.6	28.9 ±2.1	29.3 ±2.2	21.2–41.5†
Mean rCBV/tissue volume (ml/cm^3)	1.9 ±0.6	1.9 ±0.9	2.0 ±0.9	1.7 ±0.6	2.1 ±1.0	2.1 ±0.9	2.0 ±0.9	1.2– 2.0‡
Mean rCBF/tissue volume (ml/min/cm^3)	55 ±22	57 ±30	60 ±29	52 ±21	60 ±30	64 ±30	56 ±28	42.3–49.8‖

* The cerebral regions are defined in Fig. 2.
† rCBF (ml/min/ml) (calculated from ‡ and ‖ below).
‡ Cerebral capillary volume (vol %) (*20,21*).
‖ rCBF (ml/min/100 gm tissue) (*18,19* and references therein).

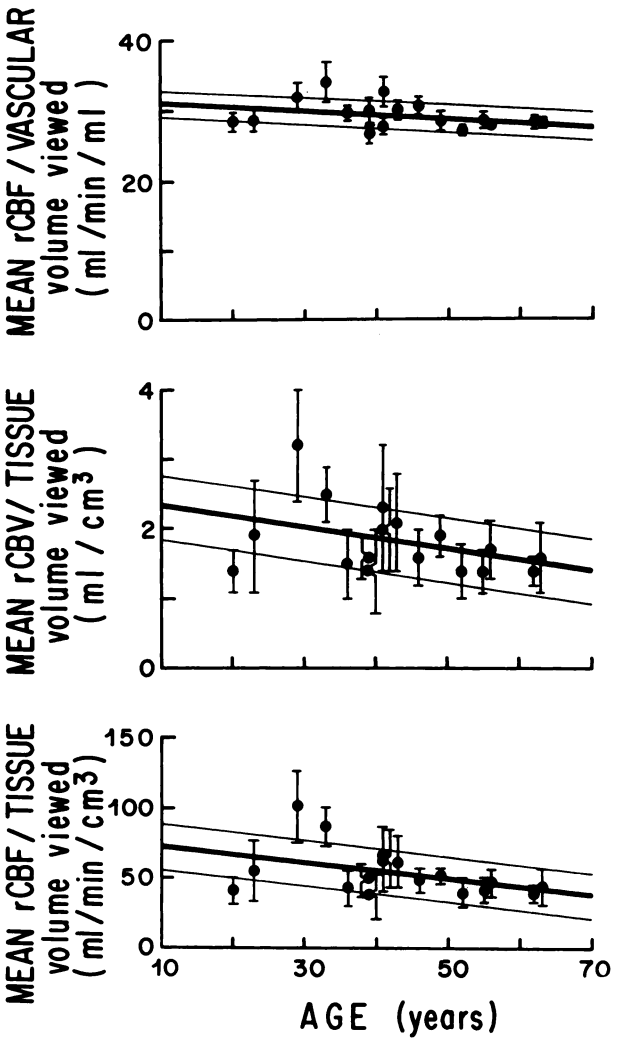

FIG. 3. Regional cerebral blood flow (rCBF) per monitored vascular volume, regional cerebral vascular volume (rCBV) and rCBF per monitored tissue volume for normal subjects as function of age of subjects. Means of values determined in six regions are plotted. Standard deviations are indicated by error bars. Unweighted linear regression analyses (heavy lines) and standard deviations (light lines) of means are also shown.

unweighted linear regression analysis of the plotted points illustrates a decrease in rCBF per monitored vascular volume with age, as might be expected from observations of circulation times with age (*3,22,23*). A similar decrease with age is observed in rCBV and in rCBF per monitored tissue volume. However, the relatively small number of measurements and the large uncertainties in the mean values do not conclusively establish this age dependence.

Table 2 summarizes the results obtained from measurements made in three selected examples of regional abnormalities noted in the clinical study (*3*). Values marked with a dagger differ by more than 2 standard deviations from normal values, as determined from Fig. 3 at an age equal to that of the patient. Differences are significant only for values of rCBF per vascular volume where the standard deviation is relatively small. Values marked with two lines differ by more than 2 standard deviations from the mean of other regional values in the same patient.

DISCUSSION

Within the limits of applicability of the chosen model, the present analysis provides values of rCBF in the monitored vascular volume as well as normal values of rCBV and rCBF in the monitored volume of tissue.

Although the analysis yields absolute flow rate and vascular volume, the model is a satisfactory representation of regional cerebral circulation only to the extent that the actual physiological phenomena are reasonably well approximated by the assumptions of the model. Further, the model is useful in the description of those pathological cases where the physiological alteration falls within the framework of the model.

It is evident that a fair appraisal of the model cannot be made solely on the basis of the 17 normal

TABLE 2. VALUES OF rCBF AND rCBV IN THREE PATIENTS

		Cerebral region					
	Pt*	AI	MI	PI	AS	MS	PS
rCBF/vascular volume (ml/min/ml)	I L	29.9	29.0	24.3†‖	29.7	27.6	‡
	II R	28.2	27.2	23.2†‖	29.1	27.7	‡
	III L	31.4	29.0	30.8	31.8	29.3	28.4
rCBV/tissue volume (ml/cm³)	I L	1.9	1.9	2.7	2.9	2.2	‡
	II R	1.4	1.6	2.2‖	1.3	1.2	‡
	III L	1.8	1.2‖	2.4	2.1	1.7	2.5
rCBF/tissue volume (ml/min/cm³)	I L	56	55	67	85	60	‡
	II R	39	45	51	40	35	‡
	III L	56	33‖	73	67	70	70

* Left (L) or Right (R) hemisphere; see ref. (3) for description of patients.
† Values differ (>±2 s.d.) from normal values (Fig. 3).
‡ No measurement obtained.
‖ Values differ (>±2 s.d.) from mean of other regional values in the same patient.

subjects and the three cases of regional abnormalities quoted. Although it is not the purpose of this paper to discuss the analysis of measurements in patients with intracranial pathology, certain features of the model may be pointed out in the three cases examined in the clinical study (*3*).

In Case I, the circulation study supplements the angiographic information by identifying a regional abnormality in the PI region adjacent to the angiographically observed abnormality. The model analysis clearly confirms this abnormality and illustrates the fact that, in this case, the rCBF per vascular volume alone (or the reciprocal of the regional mean transit time) is a sufficiently sensitive clinical index of regional cerebral circulation. If there has been a change in either rCBV or the rCBF per tissue volume, the change is too subtle to be detected in the analysis of the measurement.

In Case II, the circulation study also contributes information not otherwise obtained angiographically. The model analysis demonstrates a decrease in rCBF per vascular volume in the PI region and indicates that this is due specifically to an increase in rCBV.

Case III is perhaps an example of the virtue as well as the shortcoming of the model. The MI regional abnormality is indicated in the analysis as a decrease in rCBV and rCBF per tissue volume such that the rCBF per vascular volume remains within normal values. A decrease in rCBV confirms the observation of an increase in the width of the MI regional activity distribution and further suggests that a transit-time study alone is relatively insensitive to this type of abnormality. On the other hand, the AI regional abnormality is not confirmed in the analysis. This may be expected, however, due to the contributions to the measurement from large vessel flow, which do not satisfy the criteria of the model.

As indicated above, values of rCBF per vascular volume are determined in the analysis with less uncertainty than values of rCBV (and hence, rCBF per tissue volume). The interpretation of u/b as rCBF per vascular volume has therefore been given preference in this analysis, as opposed to the customary interpretation of mean transit time (i.e., b/u), to underscore the necessity of an independent, more precise determination of regional cerebral blood volume, in order to obtain more precise values of absolute rCBF per tissue volume from measurements made with nondiffusible tracers.

The analysis attempts to extract from clinical measurements quantities of greater physiological meaningfulness (i.e., absolute values of rCBF and regional cerebral blood volume) than the simple clinical indices described in the foregoing report (*3*). As in the analysis of measurements made with diffusible indicators (*1,2,9*) it should again be emphasized that the meaningfulness of such quantities rests on the applicability of the model and its underlying assumptions as well as on the method of analysis.

There are a number of advantages to the use of a more ideal nondiffusible tracer with a short-lived, positron-emitting radionuclide label, such as ^{15}O- or ^{11}C-carboxyhemoglobin (*24–26*): (A) An independent measurement of regional cerebral blood volume may be obtained (*27,28*); (B) The extracranial measurement of regional cerebral activity distributions may be made with a lower radiation dose to the patient, as well as with greater statistical precision (*24*). Such measurements will be of greater value in the present analytical method in that absolute rCBF and rCBV can be determined with greater precision; (C) Such measurements will therefore permit a more critical examination of the applicability of the present model and analytical method to the study of regional cerebral circulation; (D) The high spatial resolution capabilities of positron annihilation coincidence detection systems (*29*) will, in addition, permit a more detailed study of regional cerebral circulation, particularly with the use of other ^{15}O-labeled compounds (*24*).

SUMMARY

Clinical measurements of regional cerebral circulation in man have been made (*3*) by extracranial monitoring of the passage of a nondiffusible radionuclide-labeled tracer through six regions of a cerebral hemisphere following intracarotid bolus injection. The measurements obtained in 17 normal subjects and in three patients with intracranial pathology are analyzed with a stochastic model of regional cerebral circulation based upon the assumption of a random walk of tracer through regions of the cerebral vascular bed. Within the limits of applicability of the model, the analysis provides normal values of regional cerebral blood flow expressed per vascular volume monitored and per tissue volume monitored, as well as normal values of regional cerebral vascular volume. Normal values are in good agreement with values determined from the work of other investigators. Possible regional abnormal values of cerebral blood flow and blood volume are demonstrated in the patients with intracranial pathology.

ACKNOWLEDGMENT

This work was supported in part by USPHS Grants 5R01-NB05769, 5T01-GM00889, and CA-07368.

REFERENCES

1. BROCK M, FIESCHI C, INGVAR DH, et al: *Cerebral Blood Flow, Clinical and Experimental Results.* Berlin, Springer Verlag, 1969

2. LUYENDIJK W: Cerebral circulation. *Progess in Brain Research* vol 30. Amsterdam, Elsevier, 1968

3. OJEMANN RG, HOOP B, BROWNELL GL, et al: Extracranial measurement of regional cerebral circulation. *J Nucl Med* 12: 532–537, 1971

4. BROWNELL GL, BERMAN M, ROBERTSON JS: Nomenclature for tracer kinetics. *Int J Appl Radiat* 19: 249–262, 1968

5. MEIER P, ZIERLER KL: On the theory of the indicator-dilution method for measurement of blood flow and volume. *J Appl Physiol* 6: 731–744, 1954

6. STEPHENSON JL: Theory of the measurement of blood flow by the dilution of an indicator. *Bull Math Biophys* 10: 117–121, 1948

7. STEPHENSON JL: Theory of measurement of blood flow by dye dilution technique. *IRE Trans on Med Electronics* PGME-12: 82–88, 1958

8. SHEPPARD CW: *Basic Principles of the Tracer Method.* New York, J. Wiley, 1962, p 178

9. ZIERLER KL: Equations for measuring blood flow by external monitoring of radioisotopes. *Circ Res* 16: 309–321, 1965

10. SHEPPARD CW: Stochastic models for tracer experiments in the circulation: parallel random walks. *J Theor Biol* 2: 33–47, 1962

11. SHEPPARD CW, UFFER MB: Stochastic models for tracer experiments in the circulation. II. Serial random walks. *J Theor Biol* 22: 188–207, 1969

12. SEARS FW: *An Introduction to Thermodynamics, The Kinetic Theory of Gases, and Statistical Mechanics* 2nd ed, Reading, Addison-Wesley, 1959, p 256

13. BASSINGTHWAIGHTE JB: Circulatory transport and the convolution integral. *Mayo Clin Proc* 42: 137–154, 1967

14. MOSS SJ, HAEBERLI W: The polarization of protons scattered by carbon. *Nucl Phys* 72: 417–424, 1965

15. HOOP B, BROWNELL GL, OJEMANN RG: An analysis of regional cerebral blood flow measurements made by external monitoring of a non-diffusible radioisotope tracer. In *Methoden und Ergebnisse der Klinischen Nuklearmedizin in Diagnostik, Therapie und Forschung,* Horst W, ed, Stuttgart, FK Schattauer Verlag, 1971 (in press)

16. BURNHAM CA, ARONOW S: A magnetic tape system for tracer studies. *Proc Ann Conf Eng Med Biol* 10: 52A3, 1968

17. WILENSKY S, ASHARE AB, PIZER SM, et al: Computer processing and display of positron scintigrams and dynamic function curves. In *Medical Radioisotope Scintigraphy* vol 1, Vienna, IAEA, 1969, pp 815–827

18. MCHENRY LC, JAFFE ME, GOLDBERG HI: Regional cerebral blood flow measurement with small probes. I. Evaluation of the method. *Neurology* (Minneap.) 19: 1198–1206, 1969

19. REIVICH M: Regulation of the cerebral circulation. *Clin Neurosurg* 16: 378–418, 1969

20. LIERSE W: Die Kapillardichte im Wirbeltiergehirn. *Acta Anat* (Basel) 54: 1–31, 1963

21. LIERSE W, HORSTMANN E: Quantitative anatomy of the cerebral vascular bed with especial emphasis on homogeneity and inhomogeneity in small parts of the gray and white matter. *Acta Neurol Scand Suppl* 14: 15–19, 1965

22. OLDENDORF WH, KITANO M: Radioisotope measurement of brain blood turnover time as a clinical index of brain circulation. *J Nucl Med* 8: 570–587, 1967

23. BURKE G, HALKO A: Cerebral blood flow studies with sodium pertechnetate Tc-99m and the scintillation camera. *JAMA* 204: 109–114, 1968

24. TER-POGOSSIAN MM, EICHLING JO, DAVIS DO, et al: The measure in vivo of regional cerebral oxygen utilization by means of oxyhemoglobin labeled with radioactive oxygen-15. *J Clin Invest* 49: 381–391, 1970

25. GLASS HI, JACOBY J, WESTERMAN B, et al: Placental localization by inhalation of radioactive carbon monoxide. *J Nucl Med* 9: 468–470, 1968

26. HOOP B, WILENSKY S, BROWNELL GL: Feasibility studies of regional myocardial oxygen turnover in the anesthetized dog with ^{15}O-labeled gases and coincidence counting. In *Symposium on the Use of Cyclotrons in Medicine.* London, Medical Research Council Cyclotron Unit, Hammersmith Hospital, 1969 (unpublished)

27. RISBERG J, ANCRI D, INGVAR DH: Correlation between cerebral blood volume and cerebral blood flow in the cat. *Exp Brain Res* 8: 321–326, 1969

28. GLASS HI, BRANT A, CLARK JC, et al: Measurement of blood volume using red cells labeled with radioactive carbon monoxide. *J Nucl Med* 9: 571–575, 1968

29. BROWNELL GL, BURNHAM CA, WILENSKY S, et al: New developments in positron scintigraphy and the application of cyclotron-produced positron emitters. In *Medical Radioisotope Scintigraphy* vol 1, Vienna, IAEA, 1969, pp 163–176